Synthesis and structure of a series of new luminescent Ag–Ln coordination polymers and the influence of the introduction of an Ag(I) ion on NIR luminescence from the Ln(III) centre†

Jing Jin, Shuyun Niu,* Qian Han and Yuxian Chi

Received (in Victoria, Australia) 14th October 2009, Accepted 12th January 2010
First published as an Advance Article on the web 1st March 2010
DOI: 10.1039/b9nj00565j

A series of new Ag–Ln coordination polymers $[LnAg_5(bdc)_4]_n$ (Ln = Eu (**1**); Yb (**2**); Er (**3**); Ho (**4**); H_2bdc = 1,2-benzenedicarbolylic acid) has been synthesized by a hydrothermal method and characterized by single-crystal X-ray diffraction, elemental analysis, thermogravimetric analysis, IR spectra, UV-Vis-NIR absorption spectra and fluorescence spectra. X-ray structural investigations reveal that these polymers are isomorphous and exhibit a 2D layer structure formed by a coordination bond and weak metal···metal interaction. Polymers **1–4** exhibit a characteristic emission corresponding to the Ln(III) ions in the near-infrared (NIR) region or in the visible region. Especially, the NIR emission bands of polymers **2–4** present evidently shift or splitting compared with the isolated Ln(III) ions due to formation of the Ag–Ln coordination polymer. In the Ag–Ln coordination polymer, the Ag···Ln separation is much shorter (3.71–3.75 Å), thus the d-orbital of the Ag(I) ion and f-orbital of the Ln(III) ion may interact and influence each other, which probably caused the inner levels of the Ag–Ln system to be tuned. This can have an important impact on the NIR emission band presenting shift or splitting, which can be confirmed by the UV-Vis-NIR absorption spectra. Solid **1** shows intense characteristic emissions of the Eu(III) ion in the visible region, which is attributed to sensitization from the ligands and Ag-block (Ag-ligand section).

Introduction

Near-infrared luminescent Ln(III) complexes or coordination polymers (Ln = Nd, Er, Yb and Ho) are attracting increasing attention for their potential uses in telecommunication, laser systems, medical diagnostics, fluoroimmuoassays etc.[1–8] The NIR-emitting properties of Ln(III) complexes stem from the *f–f* transition of Ln(III) ions. The intrinsic disadvantages of *f–f* transitions: (i) low absorption coefficient resulting in weak emission, which makes direct application difficult[9,10] and (ii) a narrow emission spectral band, which makes it difficult to meet the illumination requirement for broadband emission, have restricted the application of NIR-emitting Ln(III) complexes. Overcoming the inherent weakness, enhancing the luminescent coefficient and intensity as well as expanding the bandwidth of the emission band are becoming some of the challenges in the study of NIR luminescent Ln(III) complexes or coordination polymers. A suitable organic ligand with an antenna effect introduced into a Ln(III) complex can allow the intrinsic low absorption coefficient of Ln(III) ion to be effectively overcome.[11–20] Typical ligands used as an antenna, such as *β*-diketone, porphyrin, fluorescein, 8-quinoline as well as their derivatives, have demonstrated sensitization to the NIR emission of Ln(III) ions. Another new strategy used for improving NIR Ln(III) emission is to employ a transition metal complex (d-block) as a sensitizer for Ln(III) emission,[21–25] *i.e.*, choosing suitable organic ligand to bridge the d-block chromophore and Ln(III) luminophore into a *d–f* heterometallic complex to achieve sensitized NIR luminescence from Ln(III) through $d \rightarrow f$ energy transfer. In the studies of *d–f* heterometallic complexes with NIR emission, most of the work focuses on the 3*d*–4*f* system.[21,26–32] Though their structure types are relatively rich, the *d*- and *f*- metal ions are often not directly linked. However, the 4*d*–4*f* and 5*d*–4*f* heterometallic complexes, especially coordination polymers, remain less developed.[25,33–38] In order to probe further the relationship between luminescence property and structure, preparing multi-series of *d–f* heterometallic complexes with novel structures and NIR luminescence will be an important task for chemists. On the other hand, regarding the photophysical properties of NIR-emitting *d–f* complexes, the great majority are concerned with the luminescent efficiency and intensity of the Ln(III) center. However, the luminescent channel width is rarely documented, and our research group has paid much attention to this area. In view of 4*d* and 4*f* energy levels, we postulate that in a 4*d*–4*f* heterometallic complex, if the 4*d*–4*f* distance is short (short enough to be within cluster limits), an interaction and influence of the 4d orbital with the 4f orbital possibly occurs. Thus, the 4*f* energy level in a 4*d*–4*f* system can

School of Chemistry and Chemical Engineering, Liaoning Normal University, Dalian 116029, P. R. China. E-mail: syniu@sohu.com; Fax: 86-411-82156832; Tel: 86-411-82159044

† Electronic supplementary information (ESI) available: The supporting information includes the portion of structure figures and structural data of the complexes **1–4**, the emission spectra of the complexes **1–4** in the visible region, the TG curves and the IR spectra of the complexes **1–4**. CCDC reference numbers 743494–743497. For ESI and crystallographic data in CIF or other electronic format see DOI: 10.1039/b9nj00565j

probably be tuned, which will have a significant influence on the *f–f* emission band in the NIR region, that is, it probably causes the inherent *f–f* emission band to be shifted, spilt or broaden. In this way, the aim of expanding emission channel width is finally realised.[39] The postulation has been tentatively verified in a series of NIR-emitting Cd–Ln complexes prepared by our group.[35] In these Cd–Ln complexes, the *d*- and *f*-metal ions have a closer distance despite the absence of a Cd–Ln bond, thus the NIR emission band of Ln(III) differs from that of isolated Ln(III) ions. In this article, we introduce an Ag(I) ion into the Ln(III) complex, obtaining a series of novel Ag–Ln coordination polymers. The Ag(I) ion has two inherent properties:[40–42] (a) the Ag(I) ion is found to adopt a wide variety of coordination geometries (ranging from two to eight coordinate), which is very favorable for constructing *d–f* complexes abundant in coordination geometries. The profuse structure types of *d–f* complexes help us to understand the relationship between luminescence and structure. On the other hand, the minimum coordinate number of the Ag(I) ion is 2, which suggests that the Ag(I) ion is liable to form a cluster compound with the Ln(III) ion if a suitable ligand is chosen. Once the Ag–Ln cluster is formed, the direct interaction and influence of the 4d orbital of the Ag(I) ion with the 4f orbital of Ln(III) ion would cause the 4*f* energy level (especially the lower energy state) to be tuned and finally tune the NIR emission of the Ln(III) ion. This is one of the more important objects of carrying on the study of the Ag–Ln system for us. (b) The Ag(I) coordination complex usually has strong luminescence in the visible region, which may be used to sensitize the NIR luminescence from the Ln(III) ion under suitable circumstances. So, its introduction could provide a rich basis for further investigation of d-f luminescent complexes. Unfortunately, there are few reports on the Ag–Ln complex. We have so far only found ten or so reports on Ag–Ln complexes to our best knowledge.[43–55] In those Ag–Ln cases, from a structural point of view, the ligands bridging the Ln(III) and Ag(I) ions are focused on aromatic organic molecules with both N- and O-donor atoms, such as pyridine-carboxylato, dtpa (diethylenetriaminepentaacetato), imidazole–carboxylato as well as with acetato, oxalato and 1,2-benzenedicarboxylato as co-ligands. As far as the luminescence property goes, all the cases concern luminescence in the visible region, and are the luminescence of Eu–Ag complexes except for two examples of Tb–Ag complexes. No other Ag–Ln systems are documented. There is also no report of an Ag–Ln system with NIR luminescence.

We report herein a series of Ag–Ln coordination polymers with 2D extended structure, $[LnAg_5(bdc)_4]_n$ (Ln = Eu (**1**); Yb (**2**); Er (**3**); Ho (**4**); H_2bdc = 1,2-benzenedicarbolylic acid). To the best of our knowledge, this is the first Ag–Ln coordination polymer with NIR emission. Their structures were determined by single-crystal X-ray diffraction. The luminescence behavior of polymers **1–4** in the visible region or in the NIR region was investigated. The study on luminescence property shows that the introduction of the Ag(I) ion has a small effect on the luminescence from the Ln(III) centre in the visible region, however, it has much more effect on the NIR luminescence from the Ln(III) centre, manifesting the emission band shifting, splitting or broadening.

Results and discussion

Structural descriptions

Structural analysis shows that complex **1** is a coordination polymer with 2D extended structure. Its repeating unit $[EuAg_5(bdc)_4]$ (equalling the asymmetric unit in Fig. S1 in the Supporting Information†) comprises one Eu(III) ion, five crystallographically independent Ag(I) ions and four bdc^{2-} anions. The Eu(III) ion is coordinated by the eight oxygen atoms of four bdc^{2-} anions (Fig. 1a). Each of the Ag(I) ions has a coordination number of four through interaction with four oxygen atoms from four bdc^{2-} anions (Fig. 1b and Fig. S2†). The bond lengths of Eu–O and Ag–O are in the range of 2.331(4)–2.455(4) Å and 2.298(4)–2.568(4) Å, respectively (Table S1 in the Supporting Information†). The four bdc^{2-} anions bond to metal cations in two different fashions, which are described as μ_7-bdc and μ_5-bdc, respectively (Fig. 2). The structures of bdc^{2-} anions with different coordination modes are slightly different. The rotation of the C(carboxyl)–C(benzene) single bond leads to non-planarity of the carboxylic plane with

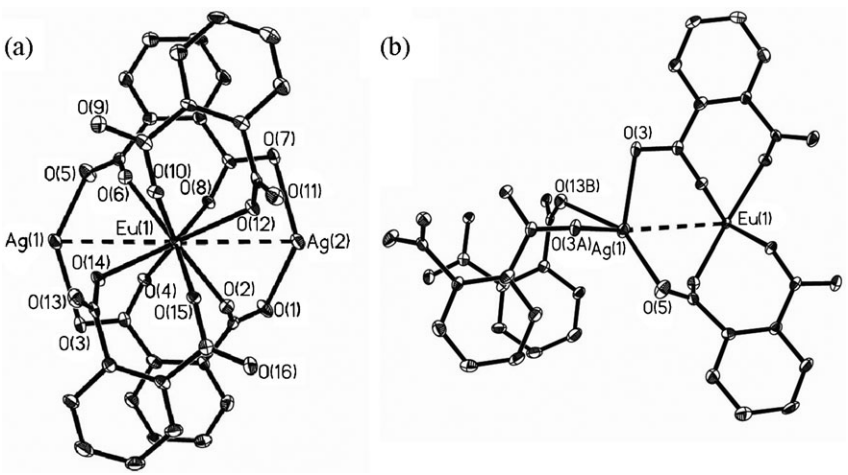

Fig. 1 Molecular structure of the local coordination around Eu(III) (a) and Ag1(I) centers (b) in **1**. The thermal ellipsoid is of 30% probability. Dashed lines represents weak M···M interactions. Symmetry code A: $-x, -y, -z + 1$; B: $-x + 1, -y, -z + 1$.

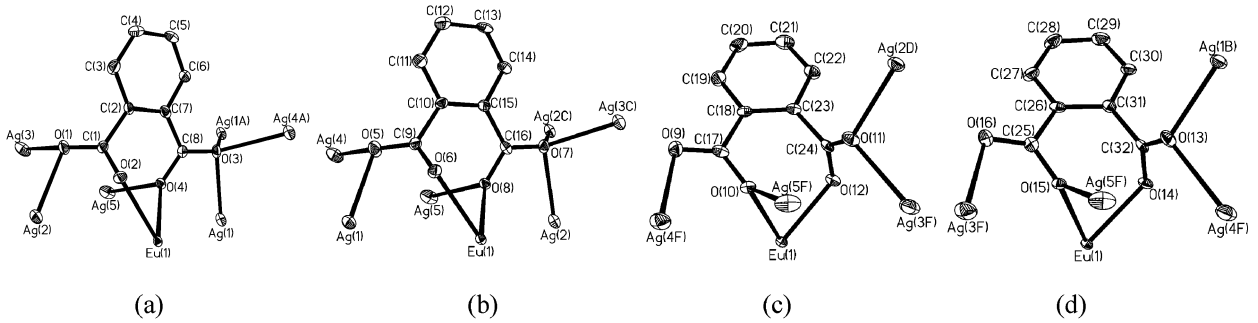

Fig. 2 The coordination mode of four bdc^{2-} anions with Eu(III) and Ag(I) ions in **1**: μ_7-bdc (a and b) and μ_5-bdc (c and d). The thermal ellipsoid is of 30% probability. Symmetry code C: $-x, -y + 1, -z$; D: $-x + 1, -y + 1, -z$; E: $x - 1, y, z$; F: $x+1, y, z$.

the phenyl plane. Moreover, the degree of rotation varies with different coordination modes (Table S2 in the Supporting Information†).

In the crystal of **1**, the Eu(III) and Ag5(I) ions are bridged by bdc^{2-} anions into 1D···Eu–O–Ag5–O–Eu–O–Ag5···chain along direction of $\vec{a}$ (Fig. 3). The Eu···Ag5 separation is 3.958(1) Å. The adjacent chains are further connected by four other Ag(I) ions coordinating to the intrachain bdc^{2-} anions (Fig. S3 in the Supporting Information†), which results in the formation of the 2D layer in the *ac* plane as shown in Fig. 4.

In comparison with the reported structure of Ag–Ln complexes,[43–55] the main structural characteristic for complex **1** is that the carboxyl oxygen atoms act as a single-atom bridge to coordinate to metal ions (bridging Eu and Ag or Ag and Ag). This causes the central metal ions to be near each other in complex **1**: the separations of Eu···Ag are 3.73 (Eu···Ag1) and 3.75 (Eu···Ag2) Å (Fig. 1a); the separations of Ag···Ag range from 3.32 to 3.46 Å (Fig. S2 and Table S3 in the Supporting Information†). Though these interactions are weak,[40] their contribution to the stabilization and photophysical property of the system is not ignored.

The structures of complexes **2**, **3** and **4** are isomorphous with that of **1**, with the corresponding Ln(III) ions taking the place of the Eu(III) ion. The bond lengths of Ln–O and Ag–O, the structural data of bdc^{2-} anions and the separations of Ln···Ag and Ag···Ag in complexes **2–4** are listed in Tables S1, S2 and S3†, respectively.

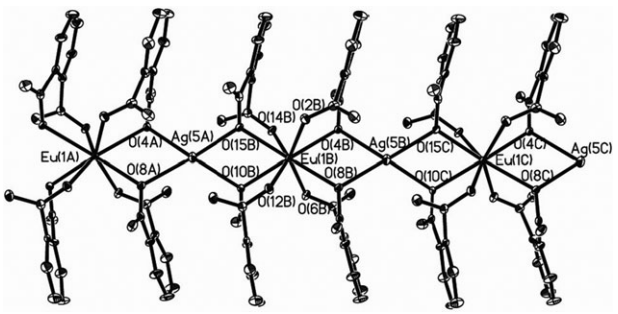

Fig. 3 The 1D chain structure along the direction of $\vec{a}$ in complex **1**. The thermal ellipsoid is of 30% probability.

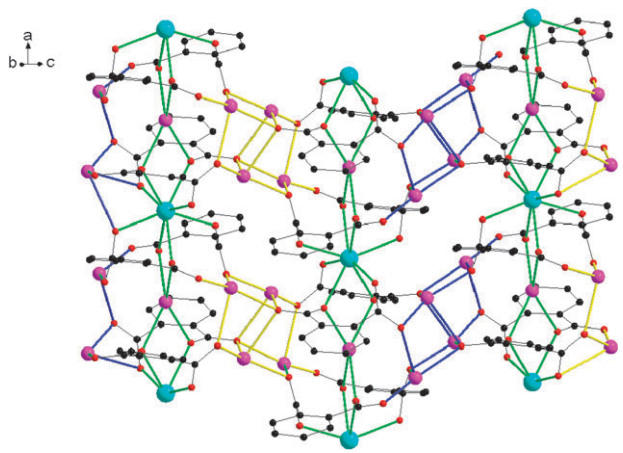

Fig. 4 Packing diagram showing a 2D layer formed in the *ac* plane of complex **1**.

Luminescent properties

At room temperature, the luminescence properties of the four complexes were investigated in the solid state. Complexes **2**, **3** and **4** show characteristic emissions of Ln(III) ions in the NIR region, complex **1** presents characteristic emissions of Eu(III) ion in the visible region.

For complex **2**, there is only one broad emission band ranging from 950 to 1050 nm (Fig. 5, λ_{max} = 998 nm), which is assigned to the $^2F_{5/2} \rightarrow {}^2F_{7/2}$ transition of the Yb(III) ion. Compared with the theoretical emission band (λ = 970 nm)[56] and that of reported Yb(III) complexes,[29,38,57,58] the emission band of complex **2** presents red-shift, which may be mainly attributed to formation of the Ag–Yb coordination polymer except for the consequence of ligand field effects. In **2**, the Ag···Yb separation is shorter (3.71 and 3.73 Å), thus, the 4d

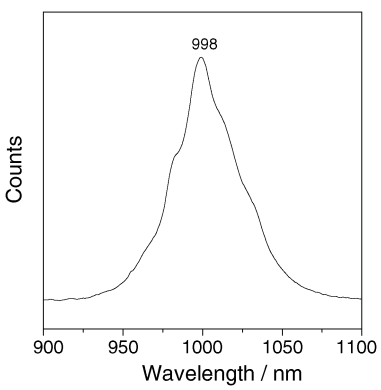

Fig. 5 The NIR emission spectrum of complex **2**.

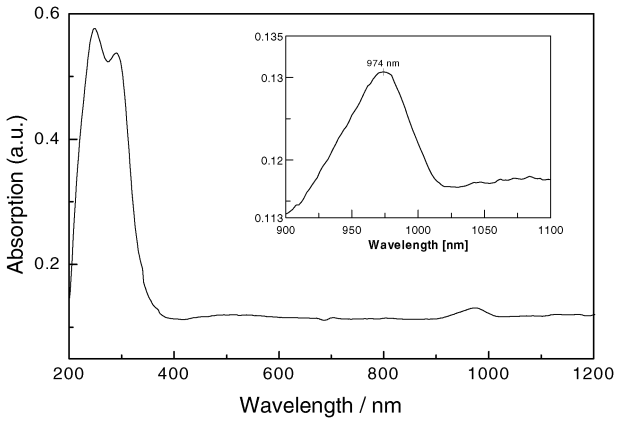

Fig. 6 The UV-Vis-NIR absorption spectra of complex **2**.

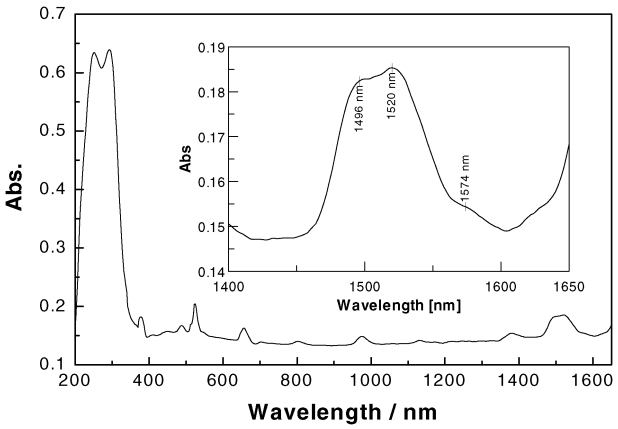

Fig. 8 The UV-Vis-NIR absorption spectra of complex **3**.

orbital of the Ag(I) ion and 4f orbital of the Yb(III) ion may interact and influence each other, which probably causes the inner levels of the system of Ag–Yb to be tuned. One result is that the energy lowers for the $^2F_{5/2}$ state of Yb(III), which can be further illustrated by the electronic absorption spectrum of complex **2** (Fig. 6). The absorption band corresponding to the $^2F_{7/2} \rightarrow {}^2F_{5/2}$ transition of the Yb(III) ion also exhibits red-shift when compared with the theoretical absorption band (970 nm). Then, when the electrons returned to the ground state, a red-shift emission band was observed.

With λ_{ex} = 380 nm, complex **3** exhibits one broad emission band extending from 1450 to 1650 nm (Fig. 7), which is attributed to the $^4I_{13/2} \rightarrow {}^4I_{15/2}$ transition of an Er(III) ion. Compared with the theoretical emission band[59] and the emission band of other Er(III) complexes reported,[58,60,61] the emission of complex **3** presents some splitting, which is mainly attributed to formation of the Ag–Er coordination polymer. In **3**, the Ag···Er separation is closer (3.72 and 3.75 Å), therefore, the interaction and influence of the 4d orbital of the Ag(I) ion with the 4f orbital of the Er(III) ion possibly occur, which probably causes the intrasystem levels to be tuned. This tuning directly affects the 4*f* level of the Er(III) ion, showing that the energy level of the emission state ($^4I_{13/2}$) of Er(III) is split, which can be confirmed by the UV-Vis-NIR absorption spectrum of complex **3** (Fig. 8). The absorption band corresponding to the $^4I_{15/2} \rightarrow {}^4I_{13/2}$ transition also shows splitting (insert of Fig. 8, splitting into 1496, 1520 and 1574 nm peaks) when compared with the theoretical absorption band[59] (1500 nm). This indicates that in complex **3** the $^4I_{13/2}$ state of the Er(III) ion is disturbed and split owing to the interaction of the 4d orbital of Ag(I) with the 4f orbital of Er(III). So, when the excited electrons (from the split $^4I_{13/2}$ state) return to the ground state ($^4I_{15/2}$ state), the corresponding emission band is observed to split.

With λ_{ex} = 670 nm, complex **4** shows two emission bands (Fig. 9). One emission band at 995 nm is assigned to the $^5F_5 \rightarrow {}^5I_7$ transition of a Ho(III) ion. The other emission bands lying at 1400–1600 nm (1425, 1476 and 1545 nm) are assigned to the same $^5F_5 \rightarrow {}^5I_6$ transition split into three components (insert of Fig. 10). The $^5F_5 \rightarrow {}^5I_6$ emission band in complex **4** shows shift and splitting when compared with the corresponding theoretical emission value (1448 nm),[59] which can be confirmed by the absorption spectrum of complex **4** (Fig. 10). The absorption band corresponding to $^5I_8 \rightarrow {}^5I_6$ transition also presents shift and splitting (insert of Fig. 10, splitting into 1152 and 1170 nm) compared with the theoretical absorption band (1172 nm),[59] which indicates that the energy level of the $^5I_6$ state is disturbed and split because the 4d orbital of Ag(I) and the 4f orbital of Ho(III) influence each other. So, when the electrons from emissive state ($^5F_5$) turn back to the $^5I_6$ states, the corresponding emission bands shows shift and splitting.

With λ_{ex} = 298 nm, complex **1** shows the characteristic emission bands of the Eu(III) ion at 574, 592, 614, 652 and

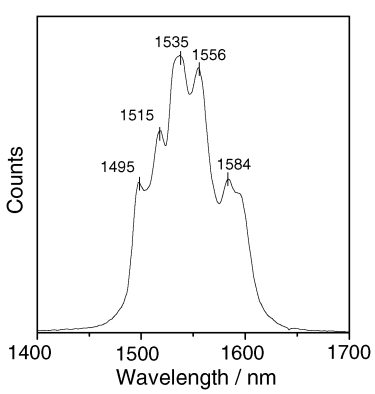

Fig. 7 The NIR emission spectrum of complex **3**.

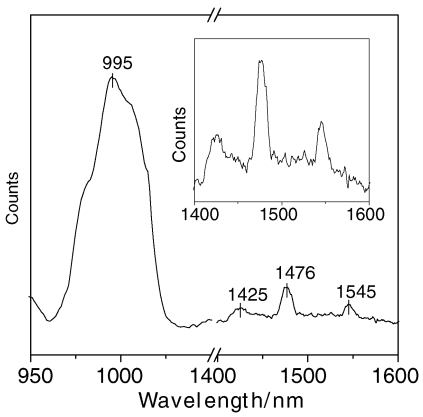

Fig. 9 The NIR emission spectrum of complex **4**.

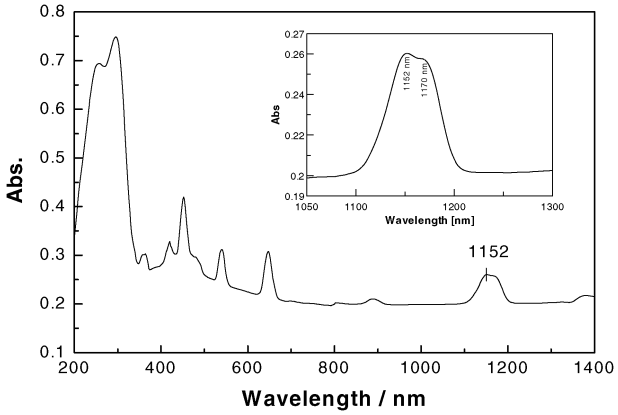

Fig. 10 The UV-Vis-NIR absorption spectra of complex **4**.

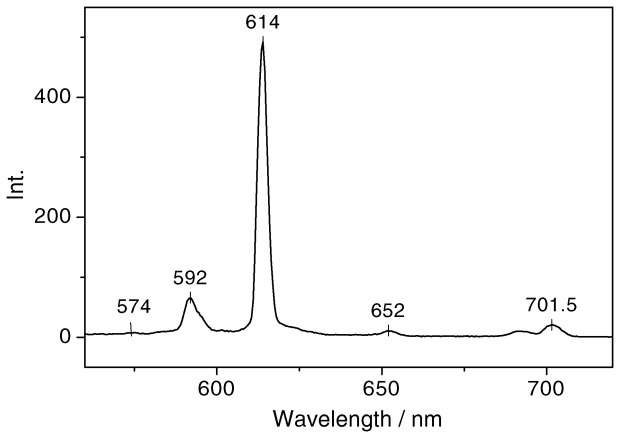

Fig. 11 The emission spectrum of complex **1**.

701.5 nm in the visible region (Fig. 11), which are assigned to the $^5D_0 \rightarrow {}^7F_J$ (J = 0, 1, 2, 3, 4) transition, respectively. The luminescence of the organic ligand and Ag-block (Ag-ligand section) is completely and incompletely quenched (Fig. S4a in the Supporting Information†), which suggests that the energy transfer from ligand and d-block to the central Eu(III) ion takes place efficiently, *i.e.*, the luminescence of Eu(III) is efficiently sensitized producing the strong *f–f* emission bands of the Eu(III) ion. However, for complexes **2–4**, the characteristic emissions of the corresponding Ln(III) ions in the visible region are very weak (Fig. S4b, S4c and S4d in the Supporting Information†). The observed emission bands are mainly due to the LLCT and LMCT transitions. This fact suggests that the energy transfer from the ligand and d-block to the f-block is less efficient in complexes **2**, **3** and **4** than that in complex **1**. Certainly, it is not ignored that the NIR emission of complexes **2–4** pass a portion of energy.

Looking at the above discussion on NIR emission spectra, it suggests that the introduction of the Ag(I) ion plays a surprising role in the NIR emission of complexes **2–4**. Namely, upon formation of the Ag–Ln coordination polymer, the Ag–Ln distance becomes much shorter. In such a way, the interaction and influence of the 4d orbital of the Ag(I) ion with the 4f orbital of the Ln(III) ions may occur, which probably causes the intrinsic 4*f* level of Ln(III) to be tuned. As a result, the NIR emission bands originating from the *f–f* transition of the Ln(III) ions show shifting, splitting or broadening. Certainly, the 4*d*–4*f* system can be further designed and optimized. This provides an approach for constructing a novel luminescent material with broadband emission. The broadband emission possesses promising applications in the following two aspects: (a) In telecommunication, since it is an essential choice to adopt NIR light as a transmitting light, the ultra-wide band luminescent material may often satisfy the need for increasing network transmission capacity. (b) Using an NIR light probe to diagnose and inspect human body disease has displayed very good value. However, in the human body different organizations and pathological focuses have differences of sensitivity to different wavelengths of light; therefore, solely using inherent emission frequency of the Ln(III) ion often cannot meet the more comprehensive diagnosis needs. Therefore, expanding the illumination wavelength width of NIR luminescent material as well as tuning the inherent illumination wavelength will open an expansive way for application of the NIR probe in medical aspects.

TG analyses

The TG analyses of all the complexes were carried out. For **1**, the TG curve (Fig. S5a in the Supporting Information†) shows that it is stable before 300 °C. The first weight loss occurs between 300 and 328 °C with a weight loss of 19.68%, which corresponds to the loss of six CO_2 molecules from the decomposition of bdc^{2-} ligands. This is in good agreement with the calculated value (19.56%). The second weight loss corresponds to the release of remaining bdc^{2-} ligands. The decomposition temperature is higher than 300 °C, which suggests that the complex **1** has good thermal stability. The TG diagram of the other three complexes are similar to that of complex **1** (Fig. S5b–d in the Supporting Information†), and all reveal two main weight losses. These results suggest that complexes **2–4** also have good thermal stability.

Conclusions

Four new Ag–Ln coordination polymers (Ln = Eu (**1**); Yb (**2**); Er (**3**); Ho (**4**)) have been first synthesized by the hydrothermal method and structurally characterized by single-crystal X-ray diffraction. These polymers are isomorphous, and there exists metal···metal interactions. A luminescence study shows that polymers **1–4** exhibit characteristic emissions corresponding to Ln(III) ions in the NIR region or in the visible region. Especially, the NIR emission bands for complexes **2–4** show shift, splitting or broadening compared with the isolated Ln(III) ions, which is attributed to formation of the Ag–Ln coordination polymer. Upon formation of the Ag–Ln coordination polymer, the Ag–Ln distance becomes much shorter (ranging from 3.71 to 3.75 Å), thus the 4d orbital of the Ag(I) ion and 4f orbital of the Ln(III) ions may interact and influence each other, which probably causes the inner levels of the Ag–Ln system to be tuned. As a result, a portion of the lower energy states of Ln(III) ions was affected to be shifted or split, which is manifested in the NIR emission spectra and UV-Vis-NIR absorption spectra. In conclusion, the introduction of an Ag(I) ion plays a surprising role in complexes **1–4**, *i.e.*, it not only contributes to the construction of an Ag–Ln

coordination polymer but also tunes the inner levels of the Ag–Ln system. In addition, it helps to sensitize the luminescence of Eu(III) ions. Further research will be focused on the preparation of an Ag–Ln cluster with suitable ligands.

Experimental

Materials and instrumentation

The salt of $Ln(NO_3)_3{\cdot}nH_2O$ was prepared by dissolving the corresponding lanthanide oxide compound (purity is 99.99%) in excess nitric acid and then naturally crystallizing. The water used was deionized water, other starting materials and reagents were all AR and used as purchased. Elemental analyses were performed on a PE-240C elemental analyzer and PLASMA-II ICP instrument. The crystal structures were determined with Bruker Smart APEX-II CCD (complex **1**) and Rigaku R-AXIS RAPID (complexes **2–4**) X-ray single crystal diffractometers. The FT-IR spectra were recorded in 4000–220 cm^{-1} scopes on a JASCO FT-480 spectrometer with a pressed KBr pellets technique. The diffuse reflectance absorption spectra were obtained in 200–2500 nm scopes on a JASCO V-570 UV-Vis-NIR spectrometer. The excitation and emission spectra in the UV-Vis region were measured with a JASCO FP-6500 fluorescence spectrometer, and the NIR emission spectra were determined with an Edinburgh FLS-920 combined time-resolved and steady-state fluorescence spectrometer with a Xe lamp as the light source and a Ge detector. Thermogravimetric (TG) analyses were carried out under a N_2 atmosphere on a Perkin-Elmer Pyris Diamond TG/DTA instrument with a heating rate of 10 °C min^{-1}.

Syntheses of the complexes

$[EuAg_5(bdc)_4]_n$ 1. $Eu(NO_3)_3{\cdot}6H_2O$ (0.2230 g, 0.5 mmol) was dissolved in water (10.0 mL, 556 mmol), to which a mixture of 1,2-H_2bdc (0.0831 g, 0.5 mmol) and ethanol (15.0 mL, 257 mmol) was added. Then, to the resulting clear solution was added in turn $AgNO_3$ (0.0831 g, 0.5 mmol) and H_2NCH_2COOH (0.3753 g, 0.5 mmol). An appropriate amount of 1.0 M NaOH solution was added dropwise to the final solution under stirring to adjust the pH value to approximately 5. Then the solution was stirred for 10 min and transferred into a Teflon bottle sealed in an autoclave, which was then heated at 90 °C for 120 h. After cooling to room temperature and a standing period of 2 d, the reaction solution was filtered and the filtrate was kept standing in the darkness. Several months passed, the yellow block crystals were separated by filtration, washed out with mother liquid and dried out in the air. The yield was 48% (0.0809 g) based on 1,2-H_2bdc. Calc. for $C_{32}H_{16}Ag_5O_{16}Eu$ **1**: C 28.52, H 1.20, Ag 40.02, Eu 11.28%. Found: C 28.43, H 1.24, Ag 38.44, Eu 10.86%. IR(KBr pellet,ν_{max}/cm^{-1}: 3448m, 3058w, 1607s, 1583s, 1559s, 1526vs, 1482s, 1446m, 1410vs, 1143w, 1041w, 1086w, 863m, 754m, 726m, 698m, 533w, 446w.

$[YbAg_5(bdc)_4]_n$ 2. 1,2-H_2bdc (0.0831 g, 0.5 mmol) was added to a solution of H_2O (5.0 mL, 278 mmol) and ethanol (10.0 mL, 172 mmol) and the solution stirred for 5 min. An appropriate amount of 1.0 M NaOH solution was added dropwise to the solution under stirring to adjust the pH value to approximately 7. Then, the mixture was added into a mixed solution of $Yb(NO_3)_3{\cdot}6H_2O$ (0.4671 g, 1 mmol) and H_2O (10.0 mL, 556 mmol) under stirring. To the resulting clear solution was added in turn $AgNO_3$ (0.1661 g, 1 mmol) and H_2NCH_2COOH (0.3753 g, 0.5 mmol). The final pH value of the solution is approximately 5. The solution was stirred for 20 min and transferred into a Teflon bottle sealed in an autoclave, which was then heated at 90 °C for 90 h. After cooling to room temperature and a standing period of 2 d, the solution was filtered and the filtrate was kept standing in the darkness. Several months passed, the yellow block crystals were separated by filtration, washed out with mother liquid and dried out in the air. The yield was 43% (0.0736 g) based on 1,2-H_2bdc. Calc. for $C_{32}H_{16}Ag_5O_{16}Yb$ **2**: C 28.08, H 1.18, Ag 39.40, Yb 12.64%. Found: C 28.00, H 1.22, Ag 37.84, Yb 12.17%. IR (KBr pellet, ν_{max}/cm^{-1}: 3446m, 3059w, 1607s, 1583s, 1560s, 1529vs, 1483s, 1446m, 1413vs, 1144w, 1086w, 1041w, 864m, 752m, 727m, 699m, 531w, 449w.

Complex **3** and **4** were synthesized by the same procedure as **2** except for the replacement of $Yb(NO_3)_3{\cdot}6H_2O$ with $Er(NO_3)_3{\cdot}6H_2O$ and $Ho(NO_3)_3{\cdot}6H_2O$, respectively.

$[ErAg_5(bdc)_4]_n$ 3. $Er(NO_3)_3{\cdot}6H_2O$ (0.4614 g, 1 mmol) were used. The yield was 36% (0.0613 g) based on 1,2-H_2bdc. Calc. for $C_{32}H_{16}Ag_5O_{16}Er$ **3**: C 28.20, H 1.18, Ag 39.57, Er 12.27%. Found: C 28.11, H 1.23, Ag 38.04, Er 11.81%. IR (KBr pellet, ν_{max}/cm^{-1}: 3450m, 3060w, 1607s, 1583s, 1560s, 1530vs, 1483s, 1447m, 1411vs, 1145w, 1087w, 1041w, 864m, 753m, 727m, 699m, 533w, 448w.

$[HoAg_5(bdc)_4]_n$ 4. $Ho(NO_3)_3{\cdot}6H_2O$ (0.4590 g, 1 mmol) were used. The yield was 38% (0.0646 g) based on 1,2-H_2bdc. Calc. for $C_{32}H_{16}Ag_5O_{16}Ho$ **4**: C 28.25, H 1.19, Ag 39.64, Ho 12.12%. Found: C 28.16, H 1.23, Ag 38.06, Ho 11.67%. IR(KBr pellet) ν_{max}/cm^{-1}: 3447m, 3058w, 1607s, 1583s, 1560s, 1528vs, 1482s, 1446m, 1410vs, 1142w, 1042w, 1086w, 862m, 753m, 727m, 699m, 532w, 447w. The IR spectra of complexes **1–4** are given in the Supporting Information (Fig. S6).†

Single-crystal structural determinations

X-ray single-crystal diffraction data for complexes **1** were collected on a Bruker Smart APEX-II CCD diffractometer at 293(2)K with Mo-Kα radiation (λ = 0.71073 Å) by ω scan mode. X-ray intensities of complex **2–4** were collected using a Rigaku R-AXIS RAPID IP area detector equipped with graphite-monochromated Mo-Kα radiation (λ = 0.71073 Å) at 293(2) K. Empirical absorption corrections were applied to the data using the SADABS program.[62] Structures were solved by the direct method and refined by full-matrix least squares on F^2 using the SHELXTL version 5.1.[63] All of the non-hydrogen atoms were refined anisotropically. The hydrogen atoms were included using mixed methods. The crystallographic data and structural refinement parameters of complexes **1–4** are summarized in Table 1. For complex **2**, because its crystal quality is not good, this may lead to the non-positive-definite anisotropic displacement parameters of atom C24. Therefore, the C24 atom is allowed an isotropic vibration parameter in the final refinement. In addition, for the large density maxima and minima in the final difference maps for

Table 1 Crystallographic data and structure refinement parameters for complexes **1–4**

Complex	**1**	**2**	**3**	**4**
Empirical formula	$C_{32}H_{16}Ag_5O_{16}Eu$	$C_{32}H_{16}Ag_5O_{16}Yb$	$C_{32}H_{16}Ag_5O_{16}Er$	$C_{32}H_{16}Ag_5O_{16}Ho$
Fw	1347.76	1368.84	1363.06	1360.73
T/K	293(2)	293(2)	293(2)	293(2)
λ [Å]	0.71073	0.71073	0.71073	0.71073
Crystal system	Triclinic	Triclinic	Triclinic	Triclinic
Space group	$P\bar{1}$	$P\bar{1}$	$P\bar{1}$	$P\bar{1}$
a/Å, α (°)	7.9028(11), 63.459(1)	7.816(5), 63.78(3)	7.8516(16), 63.69(3)	7.858(5), 63.63(3)
b/Å, β (°)	14.954(2),81.431(2)	14.875(13), 81.62(3)	14.938(3), 81.53(3)	14.940(10), 81.49(3)
c/Å, γ (°)	15.182(2),81.284(2)	15.196(11), 81.61(3)	15.208(3), 81.41(3)	15.211(11), 81.38(2)
V/Å^3	1579.8(4)	1561.3(5)	1574.3(5)	1575.2(18)
Z	2	2	2	2
ρ/g cm^{-3}	2.833	2.912	2.875	2.869
μ/mm^{-1}	5.076	6.123	5.767	5.612
F(000)	1268	1282	1278	1276
Reflns. collected	8595	12659	12942	13022
Ind. reflns. (R_{int})	6078 (0.0202)	5793 (0.1077)	5829 (0.0671)	6081 (0.0598)
GOF on F^2	1.031	1.057	1.036	1.065
R_1, wR_2 [$I > 2\sigma(I)$]	0.0335, 0.0670	0.1043, 0.2492	0.0628, 0.1597	0.0742, 0.1950
R_1, wR_2 (all data)	0.0481, 0.0724	0.1240, 0.2639	0.0858, 0.1785	0.1000, 0.2189

complexes **2**, **3** and **4**, these maxima and minima are adjacent to the heavy atoms. CCDC-743495 (for **1**), 743494 (for **2**), 743496 (for **3**) and 743497 (for **4**) contains the supplementary crystallographic data for this paper.†

Acknowledgements

This work was supported by the National Natural Science Foundation of China (No. 20571037) and the innovational team project of Liaoning Province Educational Office (No. 2007T092).

References

1 M. Montalti, N. Zaccheroni, L. Prodi, N. O'Reilly and S. L. James, *J. Am. Chem. Soc.*, 2007, **129**, 2418.
2 J. C. G. Bünzli and C. Piguet, *Chem. Soc. Rev.*, 2005, **34**, 1048.
3 S. Quici, G. Marzanni, A. Forni, G. Accorsi and F. Barigelletti, *Inorg. Chem.*, 2004, **43**, 1294.
4 N. M. Shavaleev, S. J. A. Pope, Z. R. Bell, S. Faulkner and M. D. Ward, *Dalton Trans.*, 2003, 808.
5 S. Yanagida, Y. Hasegawa, K. Murakoshi, Y. Wada, N. Nakashima and T. Yamanaka, *Coord. Chem. Rev.*, 1998, **171**, 461.
6 C. L. Maupin, D. Parker, J. A. G. Williams and J. P. Riehl, *J. Am. Chem. Soc.*, 1998, **120**, 10563.
7 Y. Kawamaura, Y. Wada, M. Iwamuro and T. Kitamura, *Chem. Lett.*, 2000, 280.
8 L. N. Sun, H. J. Zhang, Q. G. Meng, F. Y. Liu, L. S. Fu, C. Y. Peng, J. B. Yu, G. L. Zheng and S. B. Wang, *J. Phys. Chem. B*, 2005, **109**, 6174.
9 M. Kawa and J. M. J. Fréchet, *Chem. Mater.*, 1998, **10**, 286.
10 C. Piguet, J. C. G. Bünzli, G. Bernardinelli, G. Hopfgartner and A. F. Williams, *J. Am. Chem. Soc.*, 1993, **115**, 8197.
11 S. I. Weissman, *J. Chem. Phys.*, 1942, **10**, 214.
12 N. Sabbatini, M. Guardigli and J. M. Lehn, *Coord. Chem. Rev.*, 1993, **123**, 201.
13 G. F. de Sá, O. L. Malta, C. de M. Donegá, A. M. Simas, R. L. Longo, P. A. Santa-Cruz and E. F. da Silva Jr., *Coord. Chem. Rev.*, 2000, **196**, 165.
14 S. Lis, M. Elbanowski, B. Mąkowska and Z. Hnatejko, *J. Photochem. Photobiol. A: Chem.*, 2002, **150**, 233.
15 J. Zhang, P. D. Badger, S. J. Geib and S. Petoud, *Angew. Chem., Int. Ed.*, 2005, **44**, 2508.
16 E. G. Moore, G. Szigethy, J. Xu, L. O. Pålsson, A. Beeby and K. N. Raymond, *Angew. Chem., Int. Ed.*, 2008, **47**, 9500.
17 S. Kaizaki, D. Shirotani, Y. Tsukahara and H. Nakata, *Eur. J. Inorg. Chem.*, 2005, 3503.
18 W. D. Horrocks, J. P. Bolender, W. D. Smith and R. M. Supkowski, *J. Am. Chem. Soc.*, 1997, **119**, 5972.
19 A. P. Bassett, S. W. Magennis, P. B. Glover, D. J. Lewis, N. Spencer, S. Parsons, R. M. Williams, L. De Cola and Z. Pikramenou, *J. Am. Chem. Soc.*, 2004, **126**, 9413.
20 R. F. Ziessel, G. Ulrich, L. Charbonnière, D. Imbert, R. Scopelliti and J. C. G. Bünzli, *Chem.–Eur. J.*, 2006, **12**, 5060.
21 S. I. Klink, H. Keizer and F. C. J. M. van Veggel, *Angew. Chem., Int. Ed.*, 2000, **39**, 4319.
22 D. Imbert, M. Cantuel, J. C. G. Bünzli, G. Bernardinelli and C. Piguet, *J. Am. Chem. Soc.*, 2003, **125**, 15698.
23 D. Guo, C. Y. Duan, F. Lu, Y. Hasegawa, Q. J. Meng and S. Yanagida, *Chem. Commun.*, 2004, 1486.
24 S. Torelli, D. Imbert, M. Cantuel, G. Bernardinelli, S. Delahaye, A. Hauser, J. C. G. Bünzli and C. Piguet, *Chem.–Eur. J.*, 2005, **11**, 3228.
25 M. D. Ward, *Coord. Chem. Rev.*, 2007, **251**, 1663.
26 M. Yin, X. Lei, M. Li, L. Yuan and J. Sun, *J. Phys. Chem. Solids*, 2006, **67**, 1372.
27 W. K. Wong, X. Yang, R. A. Jones, J. H. Rivers, V. Lynch, W. K. Lo, D. Xiao, M. M. Oye and A. L. Holmes, *Inorg. Chem.*, 2006, **45**, 4340.
28 W. K. Lo, W. K. Wong, J. Guo, W. Y. Wong, K. F. Li and K. W. Cheah, *Inorg. Chim. Acta*, 2004, **357**, 4510.
29 W. K. Wong, H. Liang, W. Y. Wong, Z. Cai, K. F. Li and K. W. Cheah, *New J. Chem.*, 2002, **26**, 275.
30 X. Lü, W. Bi, W. Chai, J. Song, J. Meng, W. Y. Wong, W. K. Wong and R. A. Jones, *New J. Chem.*, 2008, **32**, 127.
31 X. Yang, R. A. Jones, V. Lynch, M. M. Oye and A. L. Holmes, *Dalton Trans.*, 2005, 849.
32 Y. X. Chi, S. Y. Niu and J. Jin, *Inorg. Chim. Acta*, 2009, **362**, 3821.
33 Y. Q. Sun, J. Zhang and G. Y. Yang, *Chem. Commun.*, 2006, 4700.
34 S. G. Baca, H. Adams, D. Sykes, S. Faulkner and M. D. Ward, *Dalton Trans.*, 2007, 2419.
35 Y. X. Chi, S. Y. Niu, Z. L. Wang and J. Jin, *Eur. J. Inorg. Chem.*, 2008, 2336.
36 T. Lazarides, H. Adams, D. Sykes, S. Faulkner, G. Calogero and M. D. Ward, *Dalton Trans.*, 2008, 691.
37 H. B. Xu, L. X. Shi, E. Ma, L. Y. Zhang, Q. H. Wei and Z. N. Chen, *Chem. Commun.*, 2006, 1601.
38 H. B. Xu, L. Y. Zhang, Z. L. Xie, E. Ma and Z. N. Chen, *Chem. Commun.*, 2007, 2744.
39 M. Peng, Q. Zhao, J. Qiu and L. Wondraczek, *J. Am. Ceram. Soc.*, 2009, **92**, 542.
40 K. Nomiya, S. Takahashi, R. Noguchi, S. Nemoto, T. Takayama and M. Oda, *Inorg. Chem.*, 2000, **39**, 3301.
41 Y. Wang, L. Yi, X. Yang, B. Ding, P. Cheng, D. Z. Liao and S. P. Yan, *Inorg. Chem.*, 2006, **45**, 5822.

42 G. A. Santillan and C. J. Carrano, *Cryst. Growth Des.*, 2009, **9**, 1590.
43 D. M. L. Goodgame, T. E. Muller and D. J. Williams, *Polyhedron*, 1992, **11**, 1513.
44 N. Audebrand, J. P. Auffrédic and D. Louër, *J. Solid State Chem.*, 1997, **132**, 361.
45 C. Brouca-Cabarrecq, O. Fava and A. Mosset, *J. Chem. Crystallogr.*, 1999, **29**, 81.
46 B. Zhao, X. Y. Chen, W. Z. Wang, P. Cheng, B. Ding, D. Z. Liao, S. P. Yan and Z. H. Jiang, *Inorg. Chem. Commun.*, 2005, **8**, 178.
47 X. Gu and D. Xue, *Inorg. Chem.*, 2006, **45**, 9257.
48 X. Gu and D. Xue, *Cryst. Growth Des.*, 2006, **6**, 2551.
49 Y. Qiu, H. Liu, Y. Ling, H. Deng, R. Zeng, G. Zhou and M. Zeller, *Inorg. Chem. Commun.*, 2007, **10**, 1399.
50 Y. K. He and Z. B. Han, *Inorg. Chem. Commun.*, 2007, **10**, 1523.
51 J. X. Mou, R. H. Zeng, Y. C. Qiu, W. G. Zhang, H. Deng and M. Zeller, *Inorg. Chem. Commun.*, 2008, **11**, 1347.
52 H. Deng, Y. H. Li, Y. C. Qiu, Z. H. Liu and M. Zeller, *Inorg. Chem. Commun.*, 2008, **11**, 1151.
53 Y. K. He, H. Y. An and Z. B. Han, *Solid State Sciences*, 2009, **11**, 49.
54 Y. G. Sun, X. M. Yan, F. Ding, E. J. Gao, W. Z. Zhang and F. Verpoort, *Inorg. Chem. Commun.*, 2008, **11**, 1117.
55 X. M. Lin, Y. Ying, L. Chen, H. C. Fang, Z. Y. Zhou, Q. G. Zhan and Y. P. Cai, *Inorg. Chem. Commun.*, 2009, **12**, 316.
56 J. Y. Li, *Rare Earth Luminescent Materials and Applications*, Chemical Industry Press, Beijing, 2003, p. 8.
57 L. N. Sun, H. J. Zhang, C. Y. Peng, J. B. Yu, Q. G. Meng, L. S. Fu, F. Y. Liu and X. M. Guo, *J. Phys. Chem. B*, 2006, **110**, 7249.
58 S. Quici, M. Cavazzini, G. Marzanni, G. Accorsi, N. Armaroli, B. Ventura and F. Barigelletti, *Inorg. Chem.*, 2005, **44**, 529.
59 J. Z. Gao, Y. Wu and J. W. Kang, *Spectroscopic Properties of the Lanthanide Complexes in Aqueous Solution*, University of Electronic Science and Technology of China Publishers, Chengdu, 1995, pp. 86–101.
60 L. N. Sun, J. B. Yu, G. L. Zheng, H. J. Zhang, Q. G. Meng, C. Y. Peng, L. S. Fu, F. Y. Liu and Y. N. Yu, *Eur. J. Inorg. Chem.*, 2006, 3962.
61 P. Lenaerts, K. Driesen, R. V. Deun and K. Binnemans, *Chem. Mater.*, 2005, **17**, 2148.
62 Bruker, SMART and SAINT, Bruker AXS, Inc., Madison, Wisconsin, USA, 2002.
63 G. M. Sheldrick, *SHELXTL V5.1 Soft ware Reference Manual*, Bruker AXS, Inc., Madison, Wisconsin, USA.